Chinese Chemical Letters 36 (2025) 110149

Contents lists available at ScienceDirect

Chinese Chemical Letters

journal homepage: www.elsevier.com/locate/cclet

Structure elucidation of plumerubradins A–C: Correlations between ^{1}H NMR signal patterns and structural information of [2+2]-type cyclobutane derivatives

Yu Xiong[a,b,c,1], Li-Jun Hu[a,b,c,1], Jian-Guo Song[a,b,c], Di Zhang[a], Yi-Shuang Peng[a,b,c], Xiao-Jun Huang[a,b,c], Jian Hong[a], Bin Zhu[d,e,f,*], Wen-Cai Ye[a,b,c,*], Ying Wang[a,b,c,*]

[a] State Key Laboratory of Bioactive Molecules and Druggability Assessment, Jinan University, Guangzhou 510632, China
[b] Guangdong Province Key Laboratory of Pharmacodynamic Constituents of TCM & New Drugs Research, Guangdong-Hong Kong-Macau Joint Laboratory for Pharmacodynamic Constituents of TCM and New Drugs Research, Jinan University, Guangzhou 510632, China
[c] Center for Bioactive Natural Molecules and Innovative Drugs Research, College of Pharmacy, Jinan University, Guangzhou 510632, China
[d] State Key Laboratory of Bioreactor Engineering, East China University of Science and Technology, Shanghai 200237, China
[e] Engineering Research Centre of Pharmaceutical Process Chemistry, Ministry of Education, East China University of Science and Technology, Shanghai 200237, China
[f] Laboratory of Pharmaceutical Crystal Engineering & Technology, East China University of Science and Technology, Shanghai 200237, China

ARTICLE INFO

Article history:
Received 20 May 2024
Revised 19 June 2024
Accepted 20 June 2024
Available online 21 June 2024

Keywords:
Plumeria rubra
Cyclobutane
Biomimetic semisynthesis
MicroED
QM-HiFSA
Empirical rule for structure elucidation

ABSTRACT

[2+2]-Type cyclobutane derivatives comprise a large family of natural products with diverse molecular architectures. However, the structure elucidation of the cyclobutane ring, including its connection mode and stereochemistry, presents a significant challenge. Plumerubradins A–C (**1**–**3**), three novel iridoid glycoside [2+2] dimers featuring a highly functionalized cyclobutane core and multiple stereogenic centers, were isolated from the flowers of *Plumeria rubra*. Through biomimetic semisynthesis and chemical degradation of compounds **1**–**3**, synthesis of phenylpropanoid-derived [2+2] dimers **7**–**10**, combined with extensive spectroscopic analysis, single-crystal X-ray crystallography, and microcrystal electron diffraction experiments, the structures with absolute configurations of **1**–**3** were unequivocally elucidated. Furthermore, quantum mechanics-based ^{1}H NMR iterative full spin analysis successfully established the correlations between the signal patterns of cyclobutane protons and the structural information of the cyclobutane ring in phenylpropanoid-derived [2+2] dimers, providing a diagnostic tool for the rapid structural elucidation of [2+2]-type cyclobutane derivatives.

The [2+2]-type cyclobutane-containing natural products (CCNPs) are medicinally highly valuable and exist in various structural classes of specialized metabolites, such as alkaloids, flavonoids, stilbenes, terpenoids, and phenylpropanoids [1]. The CCNPs consist of over 300 members, all featuring a unique and highly strained cyclobutane core. These molecules are biogenetically derived from intermolecular or intramolecular [2+2] cycloaddition reactions between double bonds (generally in conjugation with chromophores) in various biogenetic precursors [1–7]. The [2+2] cycloaddition reactions enable the formation of two C–C bonds along with four new stereogenic centers in a single step with a high degree of regioselectivity and stereoselectivity, resulting in the framework variability and stereochemical diversity of the newly generated scaffolds. Compared to their biosynthetic precursors, CCNPs have a significantly expanded chemical space due to their more complex structures and multiple chiral centers [8–10]. Aside from their intriguing structural features, many CCNPs were reported to display stronger biological and pharmacological activities than their precursors [1,4].

Due to the existence of various substituents and four contiguous stereocenters in a confined space, the structure elucidation and configuration assignment of [2+2]-type cyclobutane rings present a challenging and fallible task. For [2+2]-type cyclobutane-containing dimers, the connection modes (*i.e.*, *head-to-head vs. head-to-tail*) of the two halves are commonly determined by analyzing the MS^2 fragment ions when suitable crystals for single-crystal X-ray diffraction (SCXRD) analysis are unavailable. Mean-

* Corresponding authors.
E-mail addresses: zhubin@ecust.edu.cn (B. Zhu), chywc@aliyun.com (W.-C. Ye), wangying_cpu@163.com (Y. Wang).
[1] These authors contributed equally to this work.

https://doi.org/10.1016/j.cclet.2024.110149
1001-8417/

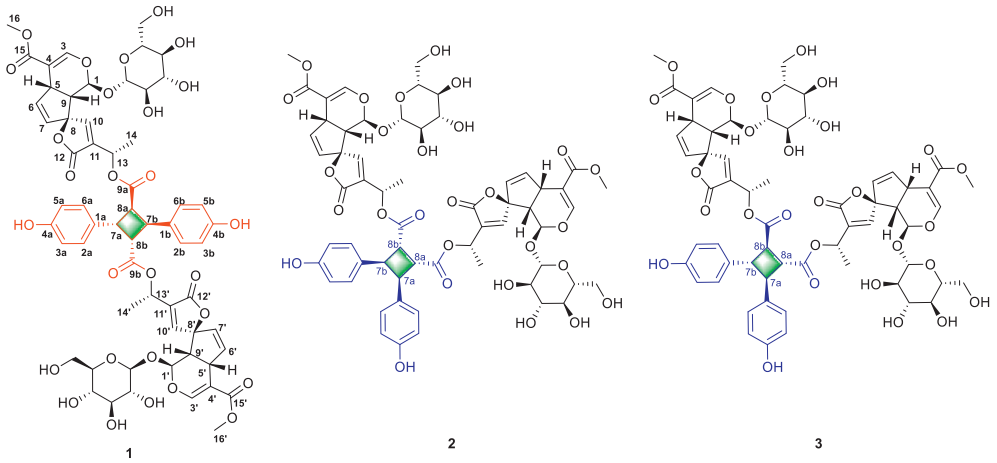

Fig. 1. Chemical structures of plumerubradins A–C (**1**–**3**).

while, the relative and absolute configuration assignments of the cyclobutane rings are usually deduced through comprehensive analysis, including 2D nuclear Overhauser effect (NOE) correlation, $^{3}J_{H,H}$ coupling constant, dihedral angle, electronic circular dichroism (ECD) curve, and density functional theory (DFT)-NMR calculation [4,11–14]. Despite the wide use of these methods, there have been misinterpretations in the stereostructures or connection modes for [2+2]-type cyclobutane-containing dimers, such as piperarborenine D [15,16], dipiperamide A [17,18], biyouyanagins A and B [19–22], and andamanicin [23,24], and they were eventually corrected through synthesis methods or SCXRD analysis. Furthermore, the stereochemistry of some reported cyclobutane-containing dimers (*e.g.*, pipernigramide E, mooniines A and B) remains unresolved [25,26]. Overall, the structure elucidation of [2+2]-type cyclobutane derivatives is a complicated and time-consuming process that requires extreme caution. Therefore, it is highly desired for the development of rapid and accurate approaches to determine the connection modes and stereochemistry of [2+2]-type cyclobutane rings.

Our group has long been focused on isolation, characterization, biomimetic synthesis and biological evaluation of natural products from Chinese medicinal plants [27–30]. In our continuing investigation, with the assistance of high performance liquid chromatography-ultraviolet detector-mass spectrometry (HPLC-UV-MS), three new [2+2] cyclobutane-containing iridoid glycoside dimers, plumerubradins A–C (**1**–**3**), together with their biogenetic precursor plumieride *p*-*E*-coumarate (**4**), were isolated from the flowers of medicinal plant *Plumeria rubra* Linn. cv. *Acutifolia* (Apocynaceae). Structurally, compounds **1**–**3** possess two rare plumeria-type iridoid glycoside units with four contiguous stereogenic centers at C-1, C-5, C-8, and C-9, as well as an isolated chiral center at C-13. The two iridoid glycoside units in compounds **1**–**3** were linked through different connection modes (*head-to-head* or *head-to-tail*) to generate phenylpropanoid-derived cyclobutane motifs with diversified stereochemistry. Despite the high complexity, the complete structures of compounds **1**–**3** (Fig. 1) including their absolute configurations were successfully established through a combination of extensive spectroscopic analysis, biomimetic semisynthesis, chemical degradation, as well as SCXRD analysis of their degradation products. In particular, the structure of compound **2** was further verified by microcrystal electron diffraction (MicroED) study at atomic resolution. Using quantum mechanics-based ^{1}H NMR iterative full spin analysis (QM-HiFSA), we gained a deeper understanding of signal patterns and coupling constants of the cyclobutane protons in synthetic phenylpropanoid-derived [2+2] dimers **7**–**10**. This analysis helped establish the correlations between the proton signal patterns and the structural information of the cyclobutane ring, including [2+2] connection modes and relative configurations. Lastly, the anti-ulcerative colitis activities of **1**–**3** were evaluated using *in vitro* unicellular (HT-29 and Caco-2 cell lines) and multicellular (Caco-2/THP-1) models.

In our initial attempts to determine the chemical structures of compounds **1**–**3**, we used comprehensive spectroscopic analyses as we described in the previous investigation for the structure elucidation of [2+2] cyclobutane-containing stilbene glycoside dimers isolated from *Polygonum multiflorum* [30]. However, due to the particular structural features of **1**–**3**, we were only able to identify their partial structures (see the Supporting information for details). Further identification was needed for the relative configuration of the isolated stereocenters (C-13 and C-13′), the [2+2] connection mode and relative configuration of the cyclobutane rings in **2** and **3**, and the absolute configurations of all the compounds.

Biogenetically, dimers **1**–**3** could be formed from two molecules of the putative biosynthetic precursor **4** *via* [2+2] cycloaddition. In order to investigate the structure further, we aimed to prepare sufficient samples of **1**–**3** using a biomimetic semisynthesis approach. We had over 3.5 g of **4**, which was isolated from *P. rubra* in the same study. Inspired by the biosynthetic hypothesis, we initially conducted the [2+2] photocycloaddition of **4** in CH_3OH or CH_3CN solution with various light sources (Table S5 in Supporting information). However, we did not obtain the desired [2+2] dimers, and in most cases, only the starting material **4** and its double bond isomerized derivative **5** were detected in the reaction mixtures. Interestingly, after testing different solvents, we discovered that when **4** was slightly or poorly dissolved in solvents such as CH_2Cl_2, THF, toluene, H_2O, and cyclohexane, the [2+2] photocycloaddition proceeded smoothly to produce the expected products **1**–**3**, along with **5**. We further optimized the reaction conditions and identified the following optimum protocol (entry 10, Table S5): suspending **4** in cyclohexane and irradiating with visible light (75 W, LED, $\lambda = 390$ nm) at room temperature for 48 h (Scheme 1); then, compounds **1**–**3** can be isolated with yields *ca.* 5%, 8%, and 3%, respectively. It is worth noting that these [2+2] photocycloadditions could also yield the products in moderate yield when water was used as the solvent (entry 9, Table S5). This suggests that those iridoid glycoside [2+2] dimers could be generated from the abundant precursor **4** in plants. The spectroscopic data of synthetic **1**–**3** were in good agreement with those of the isolated ones (Tables S6–S8 in Supporting information). It should be noted that **4** was first reported in 1983, but the stereochemistry of C-13 in **4** was still uncertain [31,32]. In this study, we determined the absolute configuration of **4** (1*S*,5*S*,8*R*,9*S*,13*S*) for the first time using chemical degra-

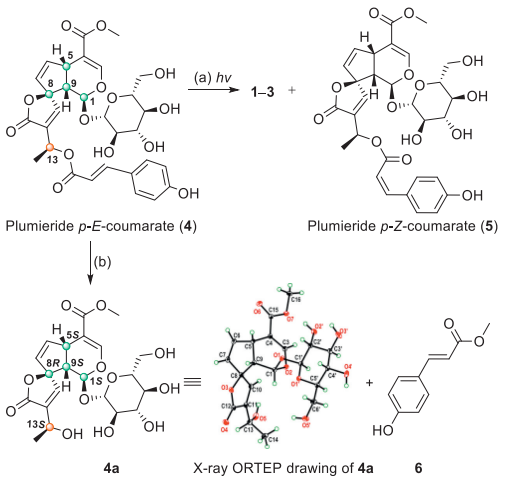

Scheme 1. Biomimetic semisynthesis of **1**–**3** and chemical degradation of **4**. Reagents and conditions: (a) **4** (0.97 mmol), cyclohexane (20 mL), N_2, room temperature, 75 W 390 nm LED, 48 h; (b) **4** (0.32 mmol), CH_3OH (25 mL), K_2CO_3 (2.60 mmol), room temperature, 5 h. LED = light-emitting diode.

dation and SCXRD analysis (Scheme 1) [Flack parameter = 0.08(10)] (CCDC: 2333495). Considering the fact that the iridoid moieties of **1**–**3** were inherited from their biosynthetic precursor **4**, therefore the absolute configurations of the two iridoid moieties in **1**–**3** were determined as 1*S*,5*S*,8*R*,9*S*,13*S* and 1′*S*,5′*S*,8′*R*,9′*S*,13′*S*, respectively.

To determine the [2+2] connection modes and relative configurations of cyclobutane motifs in **1**–**3**, a chemical degradation strategy was employed. Unfortunately, only a limited amount of simplified phenylpropanoid-derived cyclobutane methyl ester dimers of **1**–**3** were obtained, which hindered further structure elucidation. To address this, a [2+2] photocycloaddition reaction was carried out using **6** as the substrate in cyclohexane to synthesize these simplified dimers and their analogues (Fig. 2). Theoretically, eleven possible cyclobutane-containing dimers could be generated from aryl-conjugated alkene monomers *via* [2+2] photodimerization reaction (structures a–k, Fig. S9 in Supporting information) [4,33]. However, liquid chromatography-mass spectrometry (LC-MS) analysis of the reaction mixture revealed the presence of six homodimers, and only four of them (**7**–**10**) were isolated in sufficient quantities by semi-preparative HPLC with yields *ca.* 9.7%, 16.8%, 5.1%, and 3.7%, respectively. With these samples, various crystal cultivation conditions were tested to obtain single crystals of **7**–**10** for SCXRD analysis. However, despite multiple attempts, only suitable crystals of **7** were obtained. Moving forward, we prepared the 4-bromobenzoate derivatives of **8**–**10** (**8a**–**10a**) through chemical modification (Fig. 2). Fortunately, high-quality crystals of **8a**–**10a** were successfully obtained and SCXRD analysis allowed for the establishment of the structures of **7** and **8a**–**10a** (Fig. 2). Consequently, the connection modes and relative configurations of dimers **7**–**10** were unambiguously determined as: (*head-to-tail*, *syn-anti-syn-anti*), (*head-to-head*, *syn-anti-syn-anti*), (*head-to-head*, all *anti*), and (*head-to-tai*, all *anti*) (CCDC for **7** and **8a**–**10a**: 2333496, 2333494, 2333498, and 2333574), respectively. It is worth noting that the four dimeric forms represent the four predominant ones among the eleven possible structures based on the reported literatures [4,33] and the theoretical calculation results [34]. Subsequently, HPLC retention time comparison as well as co-injection analysis confirmed that **7**–**9** were the corresponding degradative cyclobutane methyl ester dimers of **1**–**3**, respectively (Fig. S10 in Supporting information). Therefore, the [2+2] cycloaddition connection modes and relative configurations of cyclobutane ring in **1**–**3** were determined to be consistent with **7**–**9**, respectively. Finally, the structures with absolute configurations of **1**–**3** were completely established.

Considering the potential risks of stereoscopic configuration inversion during the chemical degradation processes [11], we attempted to prepare single crystals of **1**–**3** for SCXRD analysis to determine their intact molecular structures. However, despite multiple attempts using various solvent systems and crystallization conditions, we did not obtain well-ordered single crystals with proper size for SCXRD analysis. Microcrystal electron diffraction (MicroED) is an emerging structure elucidation method that requires only a microcrystalline sample [35–38]. Fortunately, compound **2** was obtained as a yellow powder, which was confirmed as microcrystals through powder X-ray diffraction analysis. We then used MicroED to determine the 3D structure of compound **2**. Initially, the resolution of the acquired data for compound **2** diffracted to >2 Å on a carbon transmission electron microscope (TEM) grid, which was too poor for *ab initio* structure determination. Through further optimization of crystallization conditions, we found that slow evaporation of binary solvent system (CH_3OH-H_2O, 9:1, v/v, 2 mL) at 4 °C ultimately led to the generation of qualified microcrystals of **2** that diffracted to 1.0 Å (complete crystallographic parameters are presented in Table S22 in Supporting information). The data of five crystals were merged to provide a 1.0 Å *ab initio* solution (R_1 = 12.25%) (CCDC: 2333627). The crystal structure of compound **2** was refined anisotropically, and the asymmetric unit was plotted in Fig. 3. Finally, the absolute configuration of the cyclobutane ring in **2** was determined by using the known chiral centers of glucose residues and iridoid units as chiral references. Thus, the structure with absolute configuration of compound **2** was further confirmed by MicroED analysis, verifying the validity and reliability of the combination of spectroscopic analysis, semisynthesis, chemical degradation, and SCXRD methods for our structure elucidation. To the best of our knowledge, compound **2** is the first small-molecule natural product with a molecular weight of more than 1200 identified by MicroED [39–43]. Interestingly, an unexpected intramolecular H-bonding between 4a-OH and C-15 carbonyl was observed in the microcrystalline structure of compound **2** (Fig. S11 in Supporting information), resulting in the spatial proximity of the benzene ring and the plumeria-type iridoid unit.

As discussed above, we have successfully determined the structures with absolute configurations of the natural [2+2]-type cyclobutane-containing dimers **1**–**3** and synthetic ones **7**–**10**. Upon further analysis of their ^{1}H NMR spectra, it is interesting to point out the strong correlation between the signal patterns of the cyclobutane protons with the [2+2] connection modes and relative configurations of the cyclobutane rings (Fig. 4).

Owing to their magnetically equivalent peculiarity, the cyclobutane protons (H-7a/H-7b and H-8a/H-8b) in compound **10** exhibited a first-order spin system (A_2X_2) and appeared as two sets of triplets (t) in the ^{1}H NMR spectrum (Fig. 4D). However, in the ^{1}H NMR spectra of **7**–**9**, the cyclobutane protons displayed rather complex signal patterns, which frequently were labeled as “multiplets”, suggesting the presence of higher-order effects as described in previous studies [12,13,44–46]. To investigate the precise spin-spin coupling patterns of the cyclobutane protons in compounds **7**–**10**, a quantum mechanics-based ^{1}H iterative full spin analysis (QM-HiFSA) [47–49] was performed using Cosmic Truth (CT) software. For compound **7**, the cyclobutane protons constituted an *AA'XX'* spin system [50]. The QM-HiFSA profile of **7** revealed that H-7a/H-7b were successively coupled to H-8a (^3J = 10.52 Hz), H-8b (^3J = 7.21 Hz), and the aromatic protons [H-2a(6a) and H-2b(6b) (^4J = -0.60 Hz); H-3a(5a) and H-3b(5b) (^5J = 0.24 Hz)] (Table 1). These four spin-spin couplings theoretically would result in a “ddtt” multiplicity for the signal of H-7a/H-7b. However, due to the overlapping peaks, a *pseudo*-doublet of doublets (dd) was observed instead for H-7a/H-7b signal in the ^{1}H NMR spectrum of compound **7** (Fig. 4a). Accordingly, H-8a/H-8b signal appeared with reduced multiplicity as a doublet of dou-

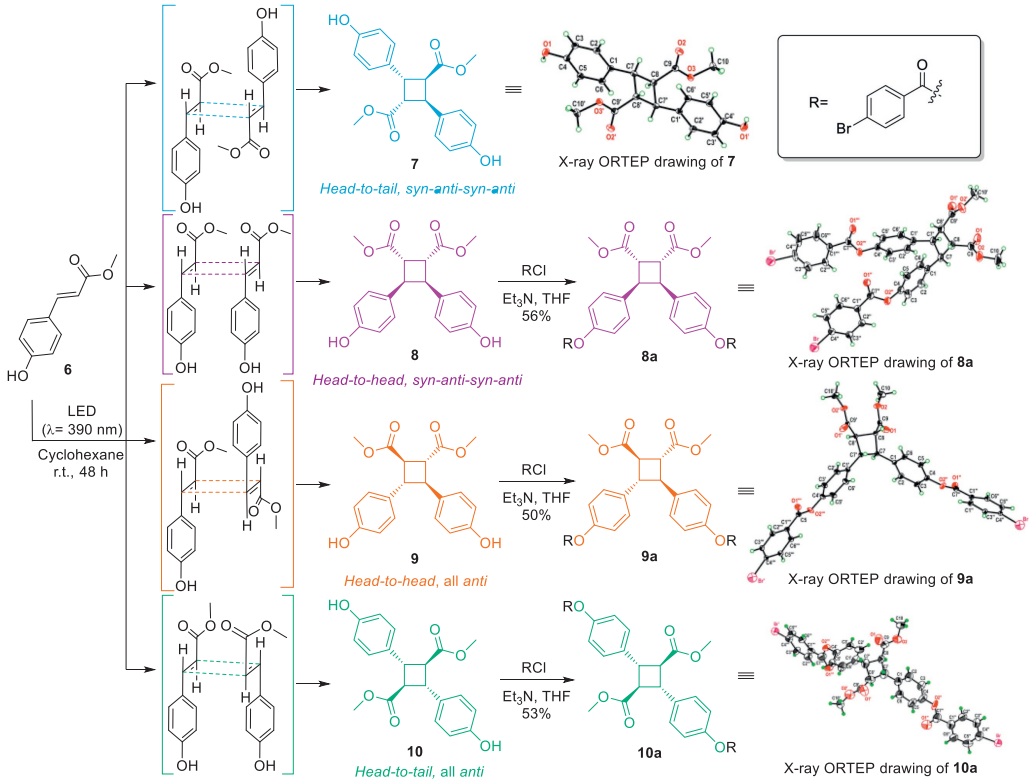

Fig. 2. Syntheses of **7**–**10** and 4-bromobenzoate derivatives **8a**, **9a**, and **10a**. THF = tetrahydrofuran.

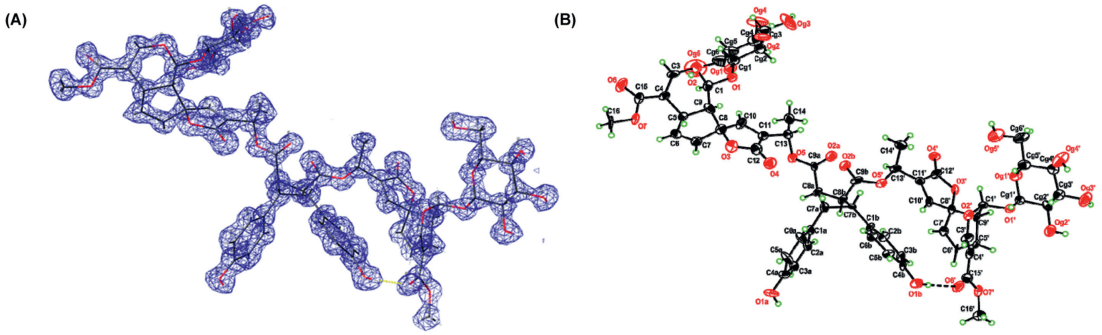

Fig. 3. Structure determination of **2** by MicroED method. (A) Corresponding electron density map superimposed on the refined structure (1.0 Å resolution). (B) Oak Ridge thermal ellipsoid plot (ORTEP) drawing of **2**.

blets, reflecting the ^3J couplings to H-7a and H-7b. Similar signal patterns were observed in the ^{1}H NMR spectrum of compound **1** (Fig. 4a). The "ddtt" multiplicity for H-7a/H-7b in compounds **8** (an *AA'XX'* system, Fig. 4b) [50] and **9** (an *AA'BB'* system, Fig. 4c) [50] could be attributed to the vicinal couplings (^3J) and the long-range couplings ($\geq^4J$) to aromatic protons (Table 1). For compounds **8** and **9**, a doublet of doublets was also observed for H-8a/H-8b. Similar signal profiles were observed in the ^{1}H NMR spectra of **2** (Fig. 4b) and **3** (Fig. 4c). Additionally, the QM-HiFSA approach also provided vicinal coupling values of cyclobutane protons in compound **10**, which were consistent with the conventional determination of J values ($^3J = 9.7$ Hz) through manual measurement (Table 1). Thus, the QM-HiFSA analysis of cyclobutane protons in compounds **7**–**10** enabled the precise determination of their ^{1}H NMR splitting patterns and spin-spin coupling patterns, leading to an in-depth understanding of the observed "multiplets". We summarized the correlations between ^{1}H NMR signal patterns and the structural information of cyclobutane rings in compounds **7**–**10** in Table 1.

As shown in Table 1, the different connection modes and relative configurations of the cyclobutane rings in compounds **7**–**9** resulted in the distinctive multiplicities and coupling constants of the cyclobutane resonances in their ^{1}H NMR spectra. It is particularly noteworthy that the signal patterns were barely influenced by the NMR solvents (acetonitrile-d_3, chloroform-d, CD_3OD, or DMSO-d_6) and the magnetic field strength of the spectrometers (400, 500, or 600 MHz) (Fig. S12 in Supporting information). The above results strongly suggest that we may use the signal patterns of the cyclobutane protons as a diagnostic tool for the rapid structure elucidation of [2+2]-type cyclobutane-containing dimers. Particularly, the splitting patterns and coupling constants of cyclobutane protons can be accurately obtained through the online open-source QM-HiFSA tool (https://ctb.nmrsolutions.fi./).

To further explore the applicability of the diagnostic signal patterns summarized in this study, we conducted a comprehensive literature review. As a result, the connection mode and stereochemistry of the cyclobutane rings of a series of reported phenylpropanoid-derived [2+2] dimers could be quickly identified

Table 1
Correlations between the ^{1}H NMR signal patterns and the structural information of cyclobutane ring in [2+2]-type cyclobutane derivatives.

No.	Connection mode relative configuration[a]	Spin system	Peak patterns[b]	Position	Mult. (*J* in Hz)[c]	Cpd.[d]
1	*Head-to-tail*	*AA'XX'*		7a/b	ddtd (10.52, 7.21, −0.60, 0.24)	**7**
	Syn-anti-syn-anti			8a/b	dd (10.52, 7.21)	
2	*Head-to-head*	*AA'XX'*		7a/b	ddtt (7.39, 6.62, −0.56, 0.37)	**8**
	Syn-anti-syn-anti			8a/b	dd (9.03, 6.62)	
3	*Head-to-head*	*AA'BB'*		7a/b	ddtt (9.62, 9.14, −0.45, 0.40)	**9**
	All *anti*			8a/b	dd (9.62, 9.29)	
4	*Head-to-tail*	A_2X_2		7a/b	ttt (9.75, 0.30, −0.29)	**10**
	All *anti*			8a/b	t (9.75)	

[a] Structural information ([2+2] connection mode and stereochemistry of the cyclobutane ring).
[b] Signal patterns of cyclobutane protons in ^{1}H NMR spectra of the four predominant [2+2] dimeric forms.
[c] QM-HiFSA analysis of the resonances of cyclobutane protons in **7**–**10**.
[d] Corresponding synthetic [2+2]-type cyclobutane derivatives in this study.

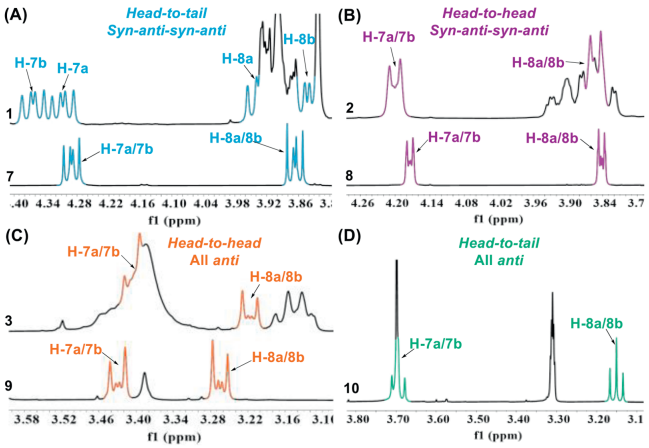

Fig. 4. Enlarged stacked ^{1}H NMR spectra of **1**–**3** and **7**–**9**: (A) Comparison of **1** and **7** in CD_3OD; (B) Comparison of **2** and **8** in CD_3OD; (C) Comparison of **3** and **9** in DMSO-d_6. (D) Enlarged ^{1}H NMR spectrum of **10** in CD_3OD. DMSO = dimethylsulfoxide.

by analyzing their ^{1}H NMR spectra using our summarized diagnostic signal patterns [12,13,33,51–53]. Additionally, we also observed similar diagnostic signal patterns in [2+2] homodimers derived from aryl-conjugated alkenes (styrenes, stilbenes, chalcones, *etc.*) [30,54–57]. Particularly, we found a strong correlation between the ^{1}H NMR profiles of cyclobutane protons in the revised structure of abrusamide A, a hydrocinnamamide-derived [2+2] homodimer with questionable original structure, and the corresponding summarized signal patterns [58,59]. These results demonstrate the feasibility of using this approach to elucidate the structures of [2+2]-type cyclobutane-containing natural products.

According to the traditional use of *P. rubra* for inflammation-related diseases in Southern China, here, we established *in vitro* ulcerative colitis (UC) model based on unicellular (HT-29 and Caco-2 cell lines) and muticellular (Caco-2/THP-1) system to explore the potential therapeutic effect of compounds **1**–**3** on UC [60]. As demonstrated in Fig. S17 (Supporting information), compound **3** significantly decreased tumor necrosis factor-α (TNF-α) expression in HT-29 monolayer model compared to control group. Meanwhile, compounds **1** and **3** both significantly downregulated the expression of pro-inflammatory cytokines [TNF-α, interleukin-6 (IL-6), IL-1β, and IL-8] in lipopolysaccharide (LPS)-stimulated Caco-2 cells and Caco-2/THP-1 co-culture model. Collectively, these results suggest that compounds **1** and **3** exhibited anti-inflammatory activities and may serve as potential therapeutic agents for UC.

In conclusion, three new iridoid glycoside [2+2] cyclobutane dimers (**1**–**3**) with unprecedented scaffolds were discovered from *P. rubra*. Compound **1** possesses a centrosymmetric phenylpropanoid-derived cyclobutane motif, compound **2** has a plane of symmetry in its phenylpropanoid-derived cyclobutane unit, and compound **3** contains a 2-fold (C_2) symmetry axis in its molecule, which posed a significant challenge for their structure elucidation. The planar structures and absolute configurations of compounds **1**–**3** were unequivocally determined by using a combination of multiple methods, including spectroscopic analysis, biomimetic semisynthesis, chemical degradation, and SCXRD analysis. In particular, the 3D structure of compound **2** was further verified using MicroED analysis, showcasing the potential of this emerging technique for elucidating the complete structure of complex natural products, including the ones with multiple stereogenic centers and highly substituted sugar moieties. Furthermore, the QM-HiFSA approach was employed to perform the complete ^{1}H NMR spectral analysis of the synthetic phenylpropanoid-derived [2+2] dimers **7**–**10**. Notably, this analysis established correlations between the structures of cyclobutane motifs and the signal patterns of cyclobutane protons, which can serve as an empirical rule for the rapid and accurate assignment of dimerization mode and stereochemistry of the cyclobutane ring in phenylpropanoid-derived [2+2] dimers, as well as other types of [2+2]-type cyclobutane-containing derivatives. Remarkably, compounds **1** and **3** demonstrated efficient amelioration of mucosal inflammation *in vitro*, highlighting their potential as therapeutic options for UC treatment.

Declaration of competing interest

The authors declare that they have no known competing financial interests or personal relationships that could have appeared to influence the work reported in this paper.

CRediT authorship contribution statement

Yu Xiong: Writing – original draft, Methodology, Investigation, Formal analysis, Data curation, Conceptualization. **Li-Jun Hu:** Writing – review & editing, Writing – original draft, Conceptualization. **Jian-Guo Song:** Writing – review & editing, Formal analysis,

Data curation. **Di Zhang:** Formal analysis, Data curation. **Yi-Shuang Peng:** Methodology, Investigation, Data curation. **Xiao-Jun Huang:** Writing – review & editing, Formal analysis, Data curation. **Jian Hong:** Writing – review & editing, Methodology. **Bin Zhu:** Writing – review & editing, Methodology, Data curation. **Wen-Cai Ye:** Writing – review & editing, Resources, Project administration. **Ying Wang:** Writing – review & editing, Resources, Project administration, Conceptualization.

Acknowledgments

This work was financially supported by the National Key R&D Program of China (No. 2023YFC3503902), the National Natural Science Foundation of China (Nos. 82293681(82293680) and 82321004), the Guangdong Basic and Applied Basic Research Foundation (Nos. 2022B1515120015 and 2021A1515111021), the Guangdong Major Project of Basic and Applied Basic Research (No. 2023B0303000026), and the Science and Technology Projects in Guangzhou (No. 202102070001). The authors are grateful to Mr. Matthias Niemitz, the founder of NMR Solutions Ltd., for granting access to Cosmic Truth software.

Supplementary materials

Supplementary material associated with this article can be found, in the online version, at doi:10.1016/j.cclet.2024.110149.

References

[1] Y.Y. Fan, X.H. Gao, J.M. Yue, Sci. China Chem. 59 (2016) 1126–1141.
[2] M.R. van der Kolk, M.A.C.H. Janssen, F.P.J.T. Rutjes, D. Blanco-Ania, ChemMedChem 17 (2022) e202200020.
[3] T. Seiser, T. Saget, D.N. Tran, et al., Angew. Chem. Int. Ed. 50 (2011) 7740–7752.
[4] P.Y. Yang, Q. Jia, S.J. Song, et al., Nat. Prod. Rep. 40 (2023) 1094–1129.
[5] V.M. Dembitsky, Phytomedicine 21 (2014) 1559–1581.
[6] B. Zhen, X.Y. Suo, J. Dang, et al., Chin. Chem. Lett. 32 (2021) 2338–2341.
[7] Y.Q. Du, L.G. Yao, X.W. Li, Y.W. Guo, Chin. Chem. Lett. 34 (2023) 107512.
[8] S. Poplata, A. Tröster, Y.Q. Zou, et al., Chem. Rev. 116 (2016) 9748–9815.
[9] D. Sarkar, N. Bera, S. Ghosh, Eur. J. Org. Chem. 10 (2020) 1310–1326.
[10] W.R. Gutekunst, P.S. Baran, J. Org. Chem. 79 (2014) 2430–2452.
[11] K.C. Nicolaou, S.A. Snyder, Angew. Chem. Int. Ed. 44 (2005) 1012–1044.
[12] Y.M. Ren, C.Q. Ke, C.P. Tang, et al., Tetrahedron Lett. 58 (2017) 2385–2388.
[13] J. Li, L.H. Tan, H. Zou, et al., J. Nat. Prod. 83 (2020) 216–222.
[14] X. Yuan, J.S. Jiang, Y.N. Yang, et al., Chin. Chem. Lett. 33 (2022) 2923–2927.
[15] I.L. Tsai, F.P. Lee, C.C. Wu, et al., Planta Med. 71 (2005) 535–542.
[16] W.R. Gutekunst, P.S. Baran, J. Am. Chem. Soc. 133 (2011) 19076–19079.
[17] S. Tsukamoto, B.C. Cha, T. Ohta, Tetrahedron 58 (2002) 1667–1671.
[18] M. Takahashi, M. Ichikawa, S. Aoyag, C. Kibayashi, Tetrahedron Lett. 46 (2005) 57–59.
[19] N. Tanaka, M. Okasaka, Y. Ishimaru, et al., Org. Lett. 7 (2005) 2997–2999.
[20] K.C. Nicolaou, D. Sarlah, D.M. Shaw, Angew. Chem. Int. Ed. 46 (2007) 4708–4711.
[21] N. Tanaka, Y. Kashiwada, S.Y. Kim, et al., J. Nat. Prod. 72 (2009) 1447–1452.
[22] K.C. Nicolaou, S. Sanchini, T.R. Wu, D. Sarlah, Chem. Eur. J. 16 (2010) 7678–7682.
[23] S. Malhotra, S.K. Koul, S.C. Taneja, et al., Phytochemistry 29 (1990) 2733–2734.
[24] R.N. Mahindru, S.C. Taneja, K.L. Dhar, R.T. Brown, Phytochemistry 32 (1993) 1073–1075.
[25] A.U. Rahman, K.F. Khattak, F. Nighat, et al., Phytochemistry 48 (1998) 377–383.
[26] H.Y. Pei, L.L. Xue, M.H. Tang, et al., J. Agric. Food Chem. 68 (2020) 2406–2417.
[27] J. Wang, J.G. Song, D.L. Zong, et al., Angew. Chem. Int. Ed. 62 (2023) e202312568.
[28] Q.F. He, Z.L. Wu, L.R. Li, et al., Angew. Chem. Int. Ed. 60 (2021) 19609–19613.
[29] L.M. Deng, L.J. Hu, Y.T.Z. Bai, et al., Org. Lett. 23 (2021) 4499–4504.
[30] S.G. Li, X.J. Huang, M.M. Li, et al., J. Nat. Prod. 81 (2018) 254–263.
[31] Y.Y. Xia, C.Z. Lin, X.J. Lu, et al., Phytochem. Lett. 25 (2018) 81–85.
[32] J.J.W. Coppen, A.L. Cobb, Phytochemistry 22 (1983) 125–128.
[33] G.L. Ma, J. Xiong, G.X. Yang, et al., J. Nat. Prod. 79 (2016) 1354–1364.
[34] A. Yaşar, N. Yaylı, A. Usta, N. Yaylı, J. Mol. Model. 16 (2010) 1347–1355.
[35] D. Shi, B.L. Nannenga, M.G. Iadanza, T. Gonen, eLife 2 (2013) e01345.
[36] B.L. Nannenga, D. Shi, A.G.W. Leslie, T. Gonen, Nat. Methods 11 (2014) 927–930.
[37] B.L. Nannenga, T. Gonen, Nat. Methods 16 (2019) 369–379.
[38] M.W. Martynowycz, M.T.B. Clabbers, J. Hattne, T. Gonen, Nat. Methods 19 (2022) 724–729.
[39] E. Danelius, S. Halaby, W.A. van der Donk, T. Gonen, Nat. Prod. Rep. 28 (2021) 421–423.
[40] E. Danelius, K. Patel, B. Gonzalez, T. Gonen, Curr. Opin. Struc. Biol. 79 (2023) 102549.
[41] T. Kunde, B.M. Schmidt, Angew. Chem. Int. Ed. 58 (2019) 666–668.
[42] L.J. Kim, M.Z. Xue, X. Li, et al., J. Am. Chem. Soc. 143 (2021) 6578–6585.
[43] J.D. Park, Y.C. Li, K. Moon, et al., Angew. Chem. Int. Ed. 61 (2022) e202114022.
[44] M. Kumar, P. Rawat, N. Rahuja, et al., Phytochemistry 70 (2009) 1448–1455.
[45] Y.S. Wang, B.T. Li, S.X. Liu, et al., J. Nat. Prod. 80 (2017) 798–804.
[46] H.J. Xie, X.Y. Chen, M.M. Li, et al., Tetrahedron Lett. 61 (2020) 151946.
[47] J.G. Napolitano, D.C. Lankin, J.B. McAlpine, et al., J. Org. Chem. 78 (2013) 9963–9968.
[48] S.X. Jing, M. Reis, Y. Alania, et al., J. Agric. Food Chem. 70 (2022) 12456–12468.
[49] Y. Tang, J.B. Friesen, D.C. Lankin, et al., J. Nat. Prod. 86 (2023) 256–263.
[50] S. Sommerwerk, R. Kluge, D. Ströhl, et al., Tetrahedron 72 (2016) 1447–1454.
[51] H.V. Stein, C.J. Berg, J.N. Maung, et al., Environ. Sci.: Processes Impacts 19 (2017) 851–860.
[52] T.B. Nguyen, A. Al-Mourabit, Photochem. Photobiol. Sci. 15 (2016) 1115–1119.
[53] R. Telmesani, S.H. Park, T. Lynch-Colameta, A.B. Beeler, Angew. Chem. Int. Ed. 54 (2015) 11521–11525.
[54] R.A. Davis, A.R. Carroll, S. Duffy, et al., J. Nat. Prod. 70 (2007) 1118–1121.
[55] Y. Liu, X.J. Zhang, N. Kelsang, et al., J. Nat. Prod. 81 (2018) 307–315.
[56] L.W. Tian, Y.J. Feng, T.D. Tran, et al., Bioorg. Med. Chem. Lett. 27 (2017) 4007–4010.
[57] M.J. Genzink, M.D. Rossler, H. Recendiz, T.P. Yoon, J. Am. Chem. Soc. 145 (2023) 19182–19188.
[58] X.J. Yuan, L. Lin, X.Q. Zhang, S.D. Deng, Phytochem. Lett. 7 (2014) 137–142.
[59] X.J. Yuan, Y.D. Liu, H. Zhao, et al., Phytochemistry 181 (2021) 112572.
[60] E.J. Wang, R. Han, M.Y. Wu, et al., Chin. Chem. Lett. 35 (2024) 108361.